Marine Chemistry 247 (2022) 104174

Contents lists available at ScienceDirect

Marine Chemistry

journal homepage: www.elsevier.com/locate/marchem

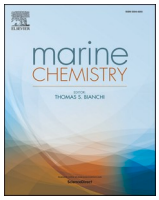

Mercury methylation linked to nitrification in the tropical North Atlantic Ocean

Lindsay D. Starr [a,*], Mark J. McCarthy [a], Chad R. Hammerschmidt [a], Ajit Subramaniam [b], Marissa C. Despins [a], Joseph P. Montoya [c], Silvia E. Newell [a]

[a] Department of Earth & Environmental Sciences, Wright State University, Dayton, OH 45435, USA
[b] Lamont-Doherty Earth Observatory, Columbia University, Palisades, New York 10964, USA
[c] School of Biological Sciences, Georgia Institute of Technology, Atlanta, GA 30332, USA

ARTICLE INFO

Keywords:
Mercury methylation rate
Nitrification rate
Amazon River plume
Nitrospina

ABSTRACT

Methylmercury (MeHg) is a toxin that poses health risks to humans and wildlife, primarily through consumption of seafood (Sunderland and Mason, 2007). Most MeHg bioaccumulation by marine fish likely occurs in the upper 200 m of the ocean, which is mostly oxygenated (Mason et al., 2012). However, mechanisms of Hg methylation in oxic seawater remain unknown, since the *hgcAB* gene cluster, which encodes proteins for MeHg production, had been found exclusively in anaerobic microbes (Gilmour et al., 2013; Parks et al., 2013). Recent work, however, has shown that *hgc* genes are widespread in oxic seawater, including in the microaerophilic nitrifier, *Nitrospina* (Tada et al., 2020; Tada et al., 2021; Gionfriddo et al., 2016; Bowman et al., 2020). Here, we show that potential MeHg production rates in Western Tropical North Atlantic Ocean surface waters, within and near the Amazon River plume, were correlated positively and strongly to nitrification rates and *Nitrospina*-specific 16S gene expression. Potential Hg methylation and nitrification rates were highest at the most saline and least turbid stations, indicating that sediment particles and nutrient-rich, riverine discharges were not the primary factors promoting either process. These novel results in oxic seawater provide further evidence that Hg methylation is linked to abundant, nitrifying microbes and may help explain marine MeHg distributions.

1. Introduction

Methylmercury is ubiquitous in the ocean, most of which is oxygenated from surface to bottom, but microbial production of MeHg is thought to be sensitive to oxygen (Lin et al., 2021; Mason et al., 2012). The presence and distribution of MeHg in oxic seawater conflicts with a long-standing paradigm that MeHg is produced only by anaerobic microbes, particularly those that reduce sulfur and iron (Gilmour et al., 2011; Monperrus et al., 2007; Gilmour et al., 2013). The only known microbes in culture that methylate Hg are anaerobic (Gilmour et al., 2011; Mason et al., 2012; Parks et al., 2013). Methylmercury production has been measured in the upper, oxic water column of the ocean (Whalin et al., 2007; Lehnherr et al., 2011; Munson et al., 2018), where it is hypothesized to occur within anoxic microzones associated with particles (Ortiz et al., 2015). Based on these measurements, and independent flux calculations based on concentration measurements (Hammerschmidt and Bowman, 2012), *in situ* production can account for >90% of MeHg in oxic surface water of the open ocean, where most seafood is harvested. However, a mechanism for MeHg production in oxic seawater remains elusive.

A variation of the Hg methylation gene (*hgc*) was recently described in the microaerophilic, nitrite-oxidizing bacteria *Nitrospina* in Antarctic sea ice (Gionfriddo et al., 2016); *Nitrospina* performs the second step of nitrification (oxidation of nitrite to nitrate, which follows oxidation of ammonium to nitrite; Santoro et al., 2010). *Nitrospina* expression of *hgc* is also widespread in the surface ocean (Villar et al., 2020), but its Hg methylating capabilities have not been confirmed, as no *hgc*-containing *Nitrospina* currently exist in culture (Tada et al., 2021). It is also unclear whether the *hgcA*-like genes in *Nitrospina* encode for a functional *Hg*-methylation protein as, since *Nitrospina*-specific *hgcA*-like genes are distinct from *hgcA* in known and predicted methylators (Gionfriddo et al., 2020).

Known Hg methylating microbes, belonging to sulfate reducing, iron reducing, and methanogenic clades (Podar et al., 2015; Christiansen et al., 2019), require anoxic conditions, but only two putative Hg methylators, *Nitrospina* and *Nitrospira*, can respire in oxic waters

* Corresponding author.
E-mail address: starr.25@wright.edu (L.D. Starr).

https://doi.org/10.1016/j.marchem.2022.104174
Received 14 March 2022; Received in revised form 15 August 2022; Accepted 2 October 2022
Available online 13 October 2022

(Gionfriddo et al., 2022). *Nitrospira*, a class of nitrite oxidizing bacteria, contains *hgcAB* genes but has only been recovered in freshwater metagenomes, not marine environments (Gionfriddo et al., 2020). Previous studies have investigated links between Hg methylation and other anaerobic reactions, such as sulfate and iron reduction in anoxic regions of the ocean, but no clear link has been shown between nitrification and Hg methylation.

We sampled water from the Western Tropical North Atlantic Ocean at six stations associated with the Amazon River plume (Fig. 1) between 18 June and 6 July 2019, during a cruise exploring the impact of the plume on planktonic productivity and communities. Stations were selected to span a gradient of planktonic productivity and surface-water salinity. Water was collected with a CTD-rosette equipped with 10-L Niskin bottles for determination of potential Hg methylation and nitrification rates, dissolved inorganic nitrogen (N) and urea concentrations, and abundance of associated genes from both surface waters (~5 m) and deep chlorophyll maxima (between 27 and 100 m depth among stations; Table 1).

2. Methods

2.1. Sample collection

Water was sampled from the Western Tropical North Atlantic Ocean at six stations associated with the Amazon River plume (Fig. 1) between 18 June and 6 July 2019 aboard the *R/V Endeavor*. Stations were selected to span a gradient of planktonic productivity and surface water salinity from international waters and territorial waters of Barbados, Suriname, and French Guiana. Temperature, dissolved oxygen, salinity, photosynthetically active radiation (PAR), turbidity (beam attenuation), and chlorophyll fluorescence were profiled with a SBE 911 CTD at each station. The CTD downcast was used to identify features (*e.g.*, deep chlorophyll maxima) in the depth profile and inform the choice of specific water sampling depths for the upward cast (Fig. 2). Water from selected depths was collected with 10-L Niskin bottles for measurement of gross potential Hg methylation and nitrification rates, as well as dissolved inorganic N and urea concentrations, from both surface water (upper 5 m) and deep chlorophyll maxima (ranging between 27 and 100 m among stations; Table 2). Experimental incubations for Hg and N transformations commenced within two hours of sampling. Water for ambient nutrient concentrations (NH_4^+, NO_3^-, NO_2^-, urea, and ortho-PO_4^{3-}) was filtered immediately upon CTD retrieval using a 60-mL syringe through a sample-rinsed, 0.22-µm Nylon syringe filter (Table 3). Filtrate was frozen promptly at −20 °C until analysis.

2.2. Nitrification rate measurements

At each station, 1 L of seawater from each sampling depth was amended with 8 µL of 10 mM 98% $^{15}NH_4Cl$ (final concentration 0.08 µM), mixed, and distributed into three 125-mL polypropylene bottles (Nalgene). Another 125-mL bottle was filled with unamended seawater as a control. Prior to incubation, initial subsamples were filtered (0.22 µm Nylon syringe filter) from amended and unamended samples into one 15-mL polypropylene tube and two 20-mL plastic scintillation vials. Incubation bottles (unamended control plus three amended) were then placed into an on-deck, flow-through incubator for ~24 h at ambient light and temperature. Samples collected from chlorophyll maxima were covered with neutral density screen to approximate *in situ* PAR intensity. After 24 h, subsamples were collected and filtered as described above for initial samples. All filtered water samples were frozen until analysis at Wright State University.

Total NH_4^+ concentrations were analyzed with a Lachat Quikchem 8500 FIA nutrient analyzer in samples (12.5 mL) collected in 15 mL polypropylene tubes. $^{15}NO_3^-$ produced *via* nitrification was reduced to $^{15}NO_2^-$ *via* Cd reductions (Newell et al., 2011; Jeffrey et al., 2012; Hampel et al., 2018) performed by transferring 25 mL of sample water from each of the two 20-mL scintillation vials into one 50-mL centrifuge tube. 100 mg of MgO, 6.6 g of NaCl, and 1 g of acidified Cd was added to each centrifuge tube. Samples were then incubated with constant, gentle agitation for ~17 h, followed by centrifugation at 1000 rpm for 15 min. The supernatant (~7.5 mL) was transferred into 12 mL Exetainers (Labco) and sealed without air headspace or bubbles. $^{15}NO_2^-$ was subsequently reduced to $^{15}N_2O$ by injecting each sample with 0.25 mL of 2 M NaN_3:20% CH_3COOH solution and incubating for 1 h at 30 °C prior to pH neutralization with 0.15 mL of 10 M NaOH (McIlvin and Altabet, 2005).

Samples were stored in the dark until analysis of $^{15}N_2O$ with a ThermoFinnigan GasBench + PreCon trace gas concentration system connected to a ThermoScientific Delta V Plus isotope-ratio mass spectrometer (Bremen, Germany) at the University of California-Davis Stable Isotope Laboratory. Nitrification rates were calculated and corrected for NaN_3 reduction efficiency based on concurrent standard reduction and the labeled fraction of the NH_4^+ pool (Hampel et al., 2020).

2.3. Hg methylation rate measurements

Four 2-L replicates of seawater were collected at each station and depth for analysis of potential Hg methylation rates. Water was amended to 10 pM Hg (final concentration; 96.41% $^{200}Hg(NO_3)_2$), which is about 10× greater than ambient total Hg concentrations in the North Atlantic mixed layer (Bowman et al., 2015). After Hg isotope

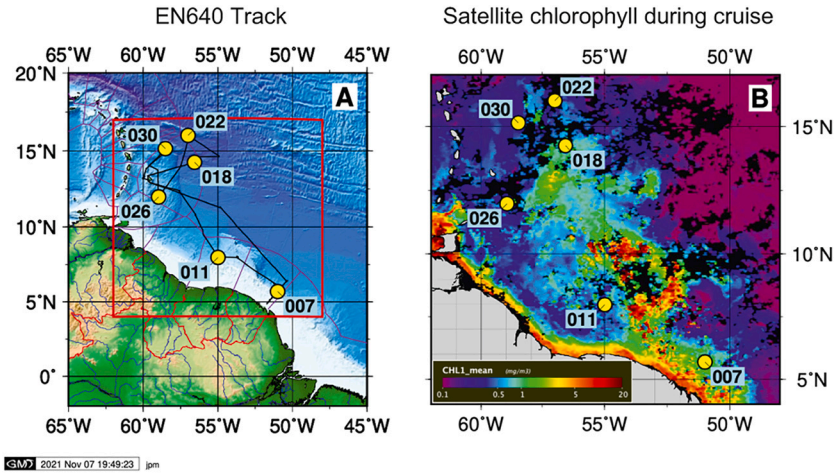

Fig. 1. (A) Stations in the North Atlantic Ocean where surface and deep chlorophyll maximum water samples were collected. Red box shows domain of (B). Monthly composite map of surface chlorophyll derived from MODIS Aqua and VIIRS sensors for June 2019. The high chlorophyll concentration shows the influence of the Amazon River outflow spreading northward. Surface waters (~5 m) ranged in salinity from 16.1 to 33.4 (Table 1). Chlorophyll satellite data obtained from *GlobColour (http://globcolour.info)* used in this study was developed, validated, and distributed by ACRI-ST, France. (For interpretation of the references to colour in this figure legend, the reader is referred to the web version of this article.)

Table 1
Amazon River plume stations, sampling date, sampling depths (m), salinity, temperature (°C), photosynthetically active radiation (PAR; W m^{-2}), beam attenuation (Beam; m^{-1}), and oxygen (μM); surface and deep chlorophyll maximum).

Station	Date	Depth	Salinity	Temperature	PAR	Beam	Oxygen
7	6/18/19	3.6	16.1	29.0	713	81	247.1
		100	36.1	28.2	17	88	189.9
11	6/21/19	3.7	33.4	27.9	392	86	196.0
		25	34.4	27.9	59	86	188.8
18	6/27/19	5.4	29.9	27.9	1145	86	203.3
		50	36.1	26.9	25	87	199.0
22	6/30/19	5.9	31.9	27.9	647	86	199.9
		74	37.2	25.8	17	87	204.6
26	7/2/19	5.7	33.2	27.9	368	86	197.4
		58	35.8	27.3	10	86	184.4
30	7/5/19	5.3	33.4	28.1	1317	85	197.5
		83	36.2	27.6	17	85	185.2

amendment, water samples were incubated in the on-deck, flow-through incubator. Water samples from deep chlorophyll maxima were covered with neutral density screen to simulate *in situ* light intensity based on PAR measurements (Table 1), and surface water was incubated without a light filter. All samples were incubated at ambient sea-surface temperature (Table 1) for ~24 h. After incubation, water was amended with $CH_3^{199}Hg$ (for isotope dilution analysis, described below) within 30 min of being removed from the incubator and promptly acidified with H_2SO_4 (1% by volume) to stop biological Hg transformations. Acidified water was analyzed for MeHg isotopes at Wright State University within three months of collection.

For analysis, acidity of water samples was titrated with 12 M KOH, buffered with 4 M acetate buffer and 0.3 mM ascorbic acid to a pH of 4.9, and derivatized with sodium tetraethylborate (Bowman and Hammerschmidt, 2011; Munson et al., 2014). Samples were then purged with N_2, and methylethylmercury (MeHg derivative) was concentrated on Tenax. Mercury isotope composition of purged MeHg was quantified with isotope-dilution gas chromatography inductively coupled plasma mass spectrometry (GC-ICPMS; Perkin Elmer Elan 9000; Hintelmann et al., 1995; Hintelmann et al., 2000). Potential Hg methylation rates were calculated from the amount of added $^{200}Hg^{2+}$ that was transformed to $CH_3^{200}Hg$ during incubation (Hintelmann and Evans, 1997). The detection limit for Hg methylation is dependent on ambient MeHg concentration, estimated from $CH_3^{202}Hg$ isotope dilution to average 0.14 ± 0.01 pM ($n = 48$), which is comparable to other measurements in the North Atlantic Ocean (Bowman et al., 2015).

2.4. Phytoplankton diagnostic pigments

Samples were collected for estimating phytoplankton pigment concentrations from the upper 100 m of the water column. Three liters of water were collected from four different depths from the surface to the deep chlorophyll maximum, according to the CTD downcast profile, and filtered (GF/F). The filters were frozen in liquid nitrogen until analysis following the HPLC method of Van Heukelem and Thomas (2001).

2.5. Nucleic acid extraction and amplification

RNA samples were collected at the surface and chlorophyll maxima at the six sites. A known volume (2–5 L) of seawater was pushed through a 0.22 μM Sterivex filter pack (Millipore). Nucleic acids were stabilized by filling the Sterivex filter with RNAlater (ThermoFisher) and stored at −80 °C until extraction.

RNA was extracted from Sterivex filters using a Rneasy Dneasy PowerWater Sterivex Kit (Qiagen) according to manufacturer instructions. Nucleic acid concentrations were measured, and RNA extract quality was assessed, using 260/280 and 260/230 ratios, with a NanoDrop Microvolume Spectrophotometer (ThermoFisher). RNA extractions were synthesized to cDNA using the ProtoScript First Strand cDNA Synthesis Kit (BioLabs), including a DNAse treatment to limit gDNA contamination. Remaining RNA extractions were stored at −80 °C for future use. cDNA was stored at −80 °C until amplification, and test amplification with PCR was used to visually confirm amplicon length *via* gel electrophoresis.

A qPCR amplification assay was completed using a Mastercycler ep Realplex2 Real-Time PCR system (Eppendorf). *Nitrospina*-specific 16S sequences were amplified using primers NitSSU_130 F (5′ -GGGTGAGTAACAC GTGAATAA-3′) and NitSSU_282 R (5'-TCAG GCCGGCTAAMCA-3′; Mincer et al., 2007). The uncultured *Nitrospinaceae* sequence EB080L20_F04 was used as a qPCR standard. The sequence underwent seven serial dilutions (10^{-4}–10^{-10} ng μL^{-1}) to create the standard curve ($R^2 > 0.99$, efficiency >85%). All samples were amplified in triplicate using the following chemical volumes: 10 μL Luna Universal qPCR Master Mix (New England BioLabs), 1 μL NitSSU_130F and NitSSU_282R, and 1 μL of standard or sample (1000–2000 ng cDNA). The total volume (20 μL) was amplified using thermal cycling parameters in Mincer et al. (2007). The qPCR reactions were completed on a single plate to avoid differences in efficiency between runs. Known *Nitrospina* have one copy of the 16S gene (Ngugi et al., 2016), but relative expression may vary from cell to cell, particularly if 16S is not constitutively expressed.

Nitrospina 16S gene copies were calculated as (ng * number mol^{-1}) / (bp * ng g^{-1} * g mol^{-1} of bp) and are reported in gene copies mL^{-1} of sample water (modified from Hampel et al., 2020). The calculated *Nitrospina* specific 16S gene copy numbers represent relative, not absolute, values, since copy numbers were normalized to the RNA concentration (ng mL^{-1} filtered) extracted from each Sterivex due to inconsistent amplification efficiency with cDNA synthesis (Newell et al., 2016).

3. Results and discussion

Potential rates of Hg methylation ranged from 0.41 to 1.29 pmol L^{-1} day^{-1} among all samples and did not differ between the upper 5 m (0.55 ± 0.15 pmol L^{-1} day^{-1}) and the chlorophyll maxima (0.69 ± 0.19 pmol L^{-1} day^{-1}; paired *t*-test, $p = 0.10$). These rates are comparable to those measured using similar techniques in the Arctic Ocean and coastal Mediterranean Sea (0.03–0.61 pmol L^{-1} day^{-1}; Monperrus et al., 2007; Lehnherr et al., 2011). Additionally, given that the added Hg substrate was 10 times higher than ambient concentrations in this study, we estimate that *in situ* rates would be about 10 times lower than the potential rates estimated here, suggesting *in situ,* gross Hg methylation rates of 0.04 to 0.13 pmol L^{-1} day^{-1}. Globally, net MeHg production in the ocean is estimated at 1–10 Mmol $year^{-1}$ or 0.005 to 0.05 pmol L^{-1} day^{-1} for net methylation rates (Hammerschmidt and Bowman, 2012; Mason et al., 2012), which include demethylation rates. Ambient MeHg concentrations were estimated from $CH_3^{202}Hg$ isotope dilution measurements (mean = 0.14 ± 0.01 pM; $n = 48$) and fall within the range of previous MeHg measurements (0.03–0.20 pM) in the equatorial Atlantic Ocean (Mason and Sullivan, 1999). Our estimated *in situ* rates imply

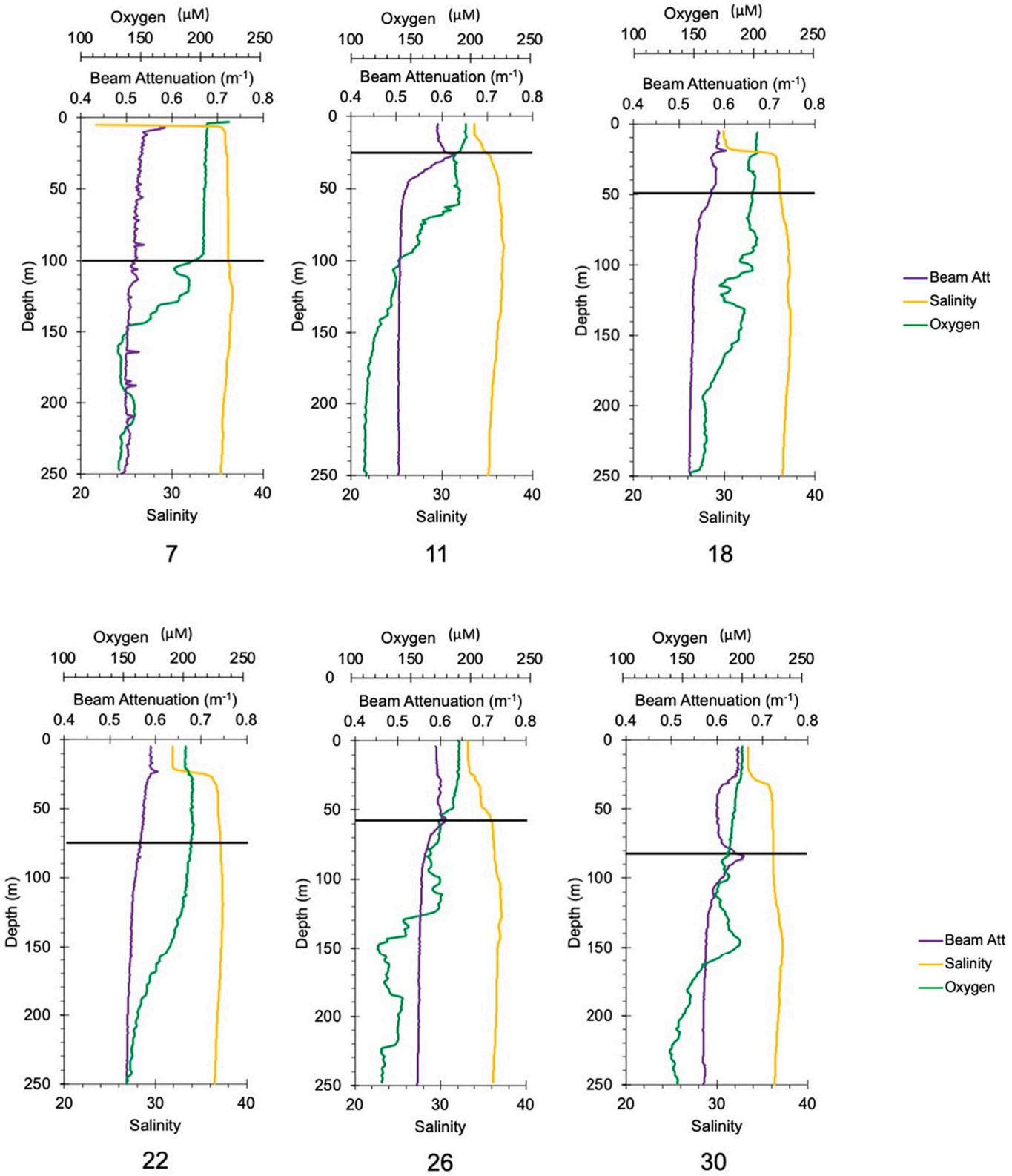

Fig. 2. Salinity, beam attenuation, and dissolved oxygen for each station. Black line indicates sampling point from the chlorophyll maximum.

turnover rates of 0.3–0.9 day^{-1} for MeHg in the upper water column of the Amazon River plume region, which are 5- to 15-fold higher than the highest turnover rates estimated for the Mediterranean Sea (Monperrus et al., 2007).

Nitrification rates in this study (0 to 292 nmol L^{-1} day^{-1}) at sites as much as 1800 km from the Amazon River mouth are up to an order of magnitude greater than rates from other studies in the oligotrophic Atlantic Ocean (0 to 12 nmol L^{-1} day^{-1}; Clark et al., 2008; Newell et al., 2013) and are more comparable to the range of rates measured at coastal shelf sites, particularly those influenced by large rivers (Bristow et al.,

Table 2
Nutrient concentrations (μM) for each station and depth (mean ± standard error of three replicate injections from a single sample, except for $n = 1$ for ortho-PO_4^{3-} at station 18). ND = not detected (detection limit for urea = 0.27 μM).

Station	Depth (m)	NH_4^+			ortho-PO_4^{3-}			NO_2^-			NO_3^-			Urea		
7	3.6	0.520	±	0.005	0.167	±	0.007	0.064	±	0.002	0.094	±	0.008	0.220	±	0.028
	100	0.930	±	0.023	0.324	±	0.004	0.196	±	0.005	0.287	±	0.004	0.433	±	0.041
11	3.7	0.856	±	0.016	0.312	±	0.003	0.143	±	0.005	0.058	±	0.002	ND		
	27	0.887	±	0.009	0.333	±	0.004	0.215	±	0.008	0.152	±	0.004	ND		
18	5.4	0.682	±	0.001	0.064			0.129	±	0.004	0.052	±	0.002	ND		
	50	0.836	±	0.006	0.030			0.156	±	0.017	0.187	±	0.002	ND		
22	5.9	0.745	±	0.013	0.284	±	0.007	0.134	±	0.014	0.061	±	0.003	ND		
	75	0.853	±	0.009	0.357	±	0.002	0.163	±	0.011	0.051	±	0.001	0.352	±	0.022
26	5.7	0.781	±	0.005	0.279	±	0.008	0.155	±	0.003	0.102	±	0.008	ND		
	58	1.227	±	0.024	0.335	±	0.014	0.265	±	0.011	0.691	±	0.005	ND		
30	5.3	0.757	±	0.011	0.313	±	0.003	0.152	±	0.003	0.066	±	0.002	ND		
	83	2.271	±	0.010	0.219	±	0.009	0.180	±	0.003	0.334	±	0.009	ND		

Table 3
Potential Hg methylation and nitrification rates (mean ± standard error; n = 3, except n = 1 for Hg methylation at station 11 surface and nitrification at station 30 surface). ND = not detected.

Station	Date	Depth	Hg Methylation rate (pmol L^{-1} day^{-1})			Nitrification rate (nmol L^{-1} day^{-1})		
7	6/18/19	3.6	0.52	±	0.14	9.8	±	10
		100	0.43	±	0.07	63	±	9
11	6/21/19	3.7	0.45			20	±	17
		25	0.41	±	0.04	67	±	20
18	6/27/19	5.4	0.49	±	0.06	ND		
		50	0.64	±	0.11	ND		
22	6/30/19	5.9	0.41	±	0.02	16	±	17
		74	0.48	±	0.11	31	±	10
26	7/2/19	5.7	0.69	±	0.26	110	±	87
		58	0.89	±	0.31	117	±	60
30	7/5/19	5.3	0.74	±	0.29	81		
		83	1.29	±	0.49	292	±	100

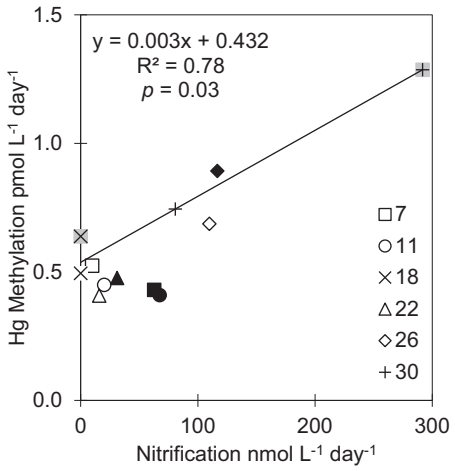

Fig. 3. Relationship between potential Hg methylation and nitrification rates in the Western Tropical North Atlantic Ocean ($p = 0.03$). Surface samples have no fill, while chlorophyll maximum samples are black or gray. Surface samples have a least squares regression of $y = 0.0026\times + 0.4492$ ($R^2 = 0.74$), and chlorophyll maximum samples have a least squares regression of $y = 0.0029\times + 0.4144$ ($R^2 = 0.77$). Similar slopes of surface and chlorophyll maximum samples suggest that the relationships are similar throughout the water column.

2015; Heiss and Fulweiler, 2016). Nitrification rates from the California Current ranged from 9 to 210 nmol L^{-1} day^{-1} (Santoro et al., 2010), similar to those from the North Atlantic equatorial current in our study. Potential nitrification rates reported here are similar in magnitude to those from an Atlantic Ocean site near the coast of Georgia (USA; 382 ± 35 nmol L^{-1} day^{-1}; Tolar et al., 2017), the Northern Gulf of Mexico coastal shelf near the Mississippi River plume (9 to 494 nmol L^{-1} day^{-1}; Bristow et al., 2015), and a coastal shelf region impacted by the Narragansett River in the northwestern Atlantic Ocean (up to 99 nmol L^{-1} day^{-1}; Heiss and Fulweiler, 2016). The consistently large range of nitrification rates across these studies suggests that coastal ocean nitrification (and nitrite oxidizers) may play a key role in global marine Hg methylation if nitrifiers are ubiquitously related to Hg methylation.

Potential Hg methylation and nitrification rates in seawater were correlated positively (Spearman's rho = 0.92; $p = 0.03$; Fig. 3), suggesting that nitrifying microbes may be an important source of MeHg in surface waters of the study area. Potential rates of Hg methylation and nitrification were highest at the most saline and least turbid stations (Stations 26 and 30; Fig. 1; Table 1; Table 3), implying that sediment particles (hotspots for anoxic microzones; Chakraborty et al., 2021) and nutrient-rich, riverine discharges were not the primary factors promoting either process. Station 30 is near a turbidity front where waters from the Amazon River have mixed extensively with offshore waters in the Atlantic Ocean (Fig. 1B). The water at station 30 has the highest surface PAR, beam attenuation, and NH_4^+ (Table 2). Accordingly, correlated rates of Hg methylation and nitrification observed in this study may be representative of ocean surface water globally.

Recent work linked Hg methylation genes and the nitrite oxidizer, *Nitrospina,* to potential MeHg production in the ocean (Villar et al., 2020; Bowman et al., 2020; Tada et al., 2020; Tada et al., 2021). The *Nitrospina*-16S gene (Hou et al., 2018) was expressed at our sampling stations (Fig. 4). There was a strong, positive correlation between expression of *Nitrospina*-16S normalized gene copies and potential Hg methylation rates ($R^2 = 0.70$, $p = 0.001$), as well as *Nitrospina*-16S and potential nitrification rates ($R^2 = 0.80$, $p = 0.0004$). However, the relationship with Hg methylation rates deteriorates if results from station 30 are excluded. Across all stations, there was no difference in *Nitrospina*-16S expression between surface and chlorophyll maximum depths ($p > 0.05$). Other microbial groups commonly found at depths where *Nitrospina* are abundant include Marine Group A, SAR324, Flavobacteria, and other 'deep' SAR11 clades (Fuhram et al., 2015; Cram et al., 2015). However, these groups are mostly chemoautotrophic and/or phototrophic bacteria and not known to be involved in nitrification MeHg cycling, so there is no obvious alternative pathway or mechanism for Hg methylation in these groups. However, without access to metagenomic data to characterize the entire microbial community, the possibility of other microbes being involved in these processes cannot be ruled out.

Our observation that potential nitrification and Hg methylation potential rates were strongly related (Spearman's rho = 0.92, $p = 0.03$; Fig. 3) suggests that *Nitrospina* may be involved in both methylating Hg and oxidizing nitrite in the oxic surface ocean near the Amazon River plume and in oxic waters underlying the plume. Our findings support previous molecular work (Villar et al., 2020; Tada et al., 2020; Tada et al., 2021) suggesting that Hg methylation may be associated with

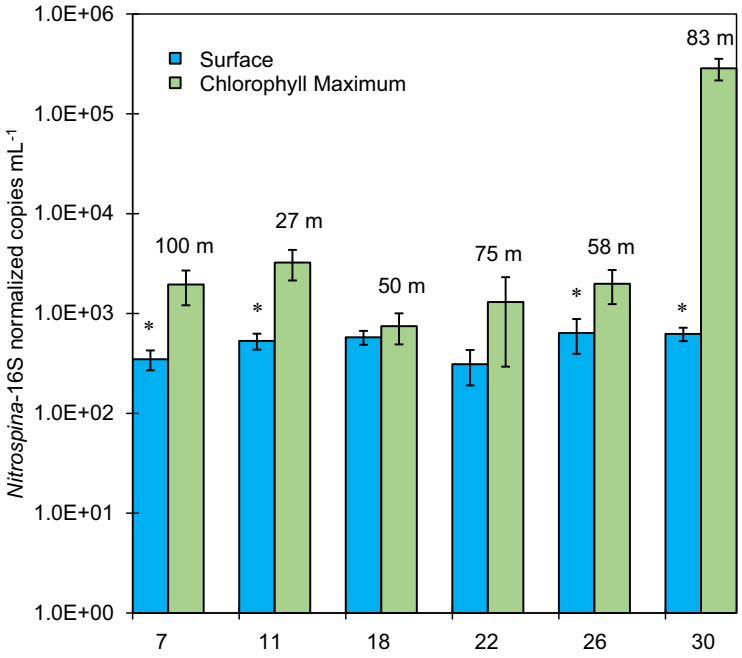

Fig. 4. Relative expression of *Nitrospina*-16S for all stations at surface and chlorophyll maxima on a log scale with standard error ($n = 3$). Gene copy numbers were normalized to the RNA extracted from each sample. Surface depth ranged from 3.6 to 5.9 m below the sea surface. Highest normalized copies were found in chlorophyll maximum samples from station 30, where highest Hg methylation and nitrification rates were found.
*Denotes difference ($p < 0.05$) between surface and deep chlorophyll maximum samples at a given station.

nitrification in the oxic surface ocean.

Since methylation rate is likely substrate limited, and Hg concentration in our incubations was elevated by an order of magnitude above ambient, we estimate an actual *in situ* production rate of 36–90 Mmol of MeHg year^{-1}. Based on the relationship in Fig. 3 and an estimated range of surface-water nitrification rates (0 to 97 nmol L^{-1} day^{-1}) in the Atlantic, Pacific, and Indian Oceans (Ward and Zafiriout, 1988; Newell et al., 2011; Grundle et al., 2013), we predict a *gross potential* production of 360–900 Mmol of MeHg year^{-1} in the open ocean. This flux is about 2- to 5-fold greater than annual Hg loadings to the surface ocean from external sources (*e.g.*, ~20 Mmol year^{-1} *via* river discharges and atmospheric deposition) and net estimated MeHg production in the ocean (1–10 Mmol year^{-1}) based on mass balances (Hammerschmidt and Bowman, 2012; Mason et al., 2012). The positive *y*-intercept of the relationship between MeHg production and nitrification (Fig. 3) suggests MeHg production from additional processes, such as sulfate- and iron-reduction in particle-associated microenvironments, or abiotic processes. The 2- to 5-fold difference between *in situ* MeHg production estimates based on our measurements and net MeHg production from mass balance is likely due in part to similarly high demethylation rates in the open ocean (Munson et al., 2018; Lehnherr et al., 2011), which is consistent with the high turnover rates implied by our data.

Both potential nitrification and Hg methylation rates were positively correlated across all stations and depths (Spearman's rho = 0.58 to 0.87) with several pigment concentrations (normalized to total chlorophyll *a*) associated with *Prochlorococcus* and eukaryotic picophytoplankton (Jeffrey et al., 2012). These pigments include divinyl chlorophyll *b*, chlorophyll *b*, and but-fucoxanthin, but these correlations were largely driven by data from the chlorophyll maxima of Stations 26 and 30 (Fig. S1). These stations were located in the northern and western reaches of the Amazon River plume, >1300–1700 km from the mouth of the river (Fig. 1). Here, the plume is diluted by mixing with seawater and is more transparent, alleviating light limitation. High rates of primary production and nitrogen fixation have been measured previously in this area of the Amazon River plume (Carpenter et al., 1999; Subramaniam et al., 2008; Montoya et al., 2019). Normalized concentrations of divinyl chlorophyll *b* and total chlorophyll *b*, diagnostic of pico-eukaryotes, were elevated at the chlorophyll maxima at these stations (Table S1; Fig. S1). Since correlations between pigments and nitrification or Hg methylation rates were driven by only two data points from Stations 26 and 30 (Fig. S1), and since phytoplankton can outcompete nitrifiers for dissolved inorganic N, we interpret these relationships with pigments to likely be coincidental and do not appear to provide an alternative explanation for the relationship between nitrification and Hg methylation (Table 3; Lomas and Lipschultz, 2006).

Several studies have suggested that particles include suboxic microhabitats, where hotspots of both nitrite oxidation and Hg methylation might occur in close proximity within an otherwise oxic water column (Date et al., 2019; Chakraborty et al., 2021; Medeiros et al., 2015; Zhang et al., 2019). However, nitrification and Hg methylation rates were not correlated with turbidity, implying that loading of terrigenous particulates and organic matter from the Amazon River were not driving either pathway. While some *Nitrospina* are microaerophilic, and all previously known pathways of Hg methylation are anaerobic, the lack of correlation with beam attenuation as a proxy for turbidity (Spearman's rho = −0.02, $p = 0.95$) is consistent with an aerobic pathway. Previous studies have also found filtered seawater (0.45 μm) can have methylation rates 1.4× higher than unfiltered samples (Munson et al., 2018).

Coupling of microbial Hg methylation and nitrification provides a possible mechanistic explanation for MeHg production in oxic waters, as well as MeHg distributions and bioaccumulation in marine systems. In addition to providing novel, process-based data, these results can also be viewed in the context of a changing marine MeHg cycle as a result of anthropogenic environmental stressors. Increased reactive N loading to the ocean is already causing coastal eutrophication and leading to increasing hypoxic zones worldwide (Falkowski et al., 2011; Peña et al., 2010). Human activities have also tripled Hg inputs to the surface ocean since industrialization (Lamborg et al., 2014). The combination of increasing substrates for nitrification and Hg methylation, development of hypoxic zones, and overall conditions favorable for Hg methylation may lead to greater MeHg bioaccumulation in seafood and, thus, human health risks.

Author contributions

LDS collected samples and measured Hg methylation and nitrification rates. MD processed nucleic acid samples and analyzed gene expression. SEN and LDS conducted statistical analyses. MJM, SEN, and

CRH conceived the project idea. AS and JPM helped collect samples and contributed pigment and CTD data. All authors contributed to data interpretations and analysis and writing of the manuscript.

Declaration of Competing Interest

Authors have no competing interests to declare.

Data availability

Data will be made available on request.

Acknowledgements

We thank the captain and crew of the *R/V Endeavor*. We thank Erica K. Strope for cruise logistics and laboratory support. Funding was provided by NSF awards to AS (OCE-1737128) and JPM (OCE-1737078) and a supplemental travel award from Wright State University to CRH.

Appendix A. Supplementary data

Supplementary data to this article can be found online at https://doi.org/10.1016/j.marchem.2022.104174.

References

Bowman, K., Collins, R. Eric, Agather, A., Lamborg, C., Hammerschmidt, C., Kaul, D., Dupont, C., Christensen, G., Elias, D., 2020. Distribution of mercury-cycling genes in the Arctic and equatorial Pacific Oceans and their relationship to mercury speciation. Limnol. Oceanogr. 65.

Bowman, K.L., Hammerschmidt, C.R., 2011. Extraction of monomethylmercury from seawater for low-femtomolar determination. Limnol. Oceanogr. Methods 9, 121–128. https://doi.org/10.4319/lom.2011.9.121.

Bowman, K.L., Hammerschmidt, C.R., Lamborg, C.H., Swarr, G., 2015. Mercury in the North Atlantic Ocean: the U.S. GEOTRACES zonal and meridional sections. Deep-Sea Res. II Top. Stud. Oceanogr. 116, 251–261. https://doi.org/10.1016/j.dsr2.2014.07.004.

Bristow, L.A., Sarode, N., Cartee, J., Caro-Quintero, A., Thamdrup, B., Stewart, F.J., 2015. Biogeochemical and metagenomic analysis of nitrite accumulation in the Gulf of Mexico hypoxic zone. Limnol. Oceanogr. 60, 1733–1750. https://doi.org/10.1002/lno.10130.

Carpenter, E.J., Montoya, J.P., Burns, J., Mulholland, M.R., Subramaniam, A., Capone, D. G., 1999. Extensive Bloom of a N 2-Fixing Diatom/Cyanobacterial Association in the Tropical Atlantic, Source: Marine Ecology Progress Series.

Chakraborty, S., Andersen, K.H., Visser, A.W., Inomura, K., Follows, M.J., Riemann, L., 2021. Quantifying nitrogen fixation by heterotrophic bacteria in sinking marine particles. Nat. Commun. 12 https://doi.org/10.1038/s41467-021-23875-6.

Christiansen, N.A., Fryirs, K.A., Green, T.J., Hose, G.C., 2019. The impact of urbanization on community structure, gene abundance and transcription rates of microbes in upland swamps of Eastern Australia. PLoS One 14.

Clark, D.R., Rees, A.P., Joint, I., 2008. Ammonium regeneration and nitrification rates in the oligotrophic Atlantic Ocean: implications for new production estimates. Limnol. Oceanogr. 53, 52–62.

Cram, J.A., Chow, C.E.T., Sachdeva, R., Needham, D.M., Parada, A.E., Steele, J.A., Fuhrman, J.A., 2015. Seasonal and interannual variability of the marine bacterioplankton community throughout the water column over ten years. ISME J. 9, 563–580.

Date, S.S., Parks, J.M., Rush, K.W., Wall, J.D., Ragsdale, S.W., Johs, A., 2019. Kinetics of enzymatic mercury methylation at nanomolar concentrations catalyzed by HgcAB. Appl. Environ. Microbiol. 85 https://doi.org/10.1128/AEM.00438-19.

Falkowski, P.G., Algeo, T., Codispoti, L., Deutsch, C., Emerson, S., Hales, B., Huey, R.B., Jenkins, W.J., Kump, R., Levin, L.A., Lyons, T.W., Nelson, N.B., Schofield, O.S., Summons, R., Talley, L.D., Thomas, E., Whitney, F., Pilcher, C.B., 2011. Ocean deoxygenation: past, present, and future. Geophys. Res. Lett. 92, 409–420. https://doi.org/10.1029/2008GL034185.

Fuhram, J.A., Cram, J.A., Needham, D.M., 2015. Marine microbial community dynamics and their ecological interpretation. Nat. Rev. Microbiol. 13, 133–146.

Gilmour, C.C., Elias, D.A., Kucken, A.M., Brown, S.D., Palumbo, A.V., Schadt, C.W., Wall, J.D., 2011. Sulfate-reducing bacterium Desulfovibrio desulfuricans ND132 as a model for understanding bacterial mercury methylation. Appl. Environ. Microbiol. 77, 3938–3951. https://doi.org/10.1128/AEM.02993-10.

Gilmour, C.C., Podar, M., Bullock, A.L., Graham, A.M., Brown, S.D., Somenahally, A.C., Johs, A., Hurt, R.A., Bailey, K.L., Elias, D.A., 2013. Mercury methylation by novel microorganisms from new environments. Environ. Sci. Technol. 47, 11810–11820. https://doi.org/10.1021/es403075t.

Gionfriddo, C.M., Tate, M.T., Wick, R.R., Schultz, M.B., Zemla, A., Thelen, M.P., Schofield, R., Krabbenhoft, D.P., Holt, K.E., Moreau, J.W., 2016. Microbial mercury methylation in Antarctic sea ice. Nat. Microbiol. 1 https://doi.org/10.1038/nmicrobiol.2016.127.

Gionfriddo, C.M., Wymore, A.M., Jones, D.S., Wilpiszeski, R.L., Lynes, M.M., Christensen, G.A., Soren, A., Gilmour, C.C., Podar, M., Elias, D.A., 2020. An improved hgcAB primer set and direct high-throughput sequencing expand Hg-Methylator diversity in nature. Front. Microbiol. 11 https://doi.org/10.3389/fmicb.2020.541554.

Gionfriddo, C.M., Capo, E., Peterson, B.D., Lin, H., Jones, D.S., Bravo, A.G., Bertilsson, S., Moreau, J., McMahon, K., Elias, D.A., Gilmour, C., 2022. Hg-MATE-Db v1.01142021: Hg-cycling Microorganisms in Aquatic and Terrestrial Ecosystems Database. https://doi.org/10.5281/ZENODO.6687122.

Grundle, D.S., Juniper, S.K., Giesbrecht, K.E., 2013. Euphotic zone nitrification in the NE subarctic Pacific: implications for measurements of new production. Mar. Chem. 155, 113–123. https://doi.org/10.1016/j.marchem.2013.06.004.

Hammerschmidt, C.R., Bowman, K.L., 2012. Vertical methylmercury distribution in the subtropical North Pacific Ocean. Mar. Chem. 132–133, 77–82. https://doi.org/10.1016/j.marchem.2012.02.005.

Hampel, J.J., McCarthy, M.J., Gardner, W.S., Zhang, L., Xu, H., Zhu, G., Newell, S.E., 2018. Nitrification and ammonium dynamics in Taihu Lake, China: seasonal competition for ammonium between nitrifiers and cyanobacteria. Biogeosciences 15, 733–748. https://doi.org/10.5194/bg-15-733-2018.

Hampel, J.J., McCarthy, M.J., Aalto, S.L., Newell, S.E., 2020. Hurricane disturbance stimulated nitrification and altered ammonia oxidizer community structure in Lake Okeechobee and St. Lucie Estuary (Florida). Front. Microbiol. 11 https://doi.org/10.3389/fmicb.2020.01541.

Heiss, E.M., Fulweiler, R.W., 2016. Coastal water column ammonium and nitrite oxidation are decoupled in summer. Estuar. Coast. Shelf Sci. 178, 110–119. https://doi.org/10.1016/j.ecss.2016.06.002.

Hintelmann, H., Evans, R.D., 1997. Application of stable isotopes in environmental tracer studies – measurement of monomethylmercury (CH3Hg+) by isotope dilution ICP-MS and detection of species transformation. Fresenius J. Anal. Chem. 358, 378–385.

Hintelmann, H., Evans, R.D., Villeneuve, J.Y., 1995. Measurement of mercury methylation in sediments by using enriched stable mercury isotopes combined with methylmercury determination by gas chromatography–inductively coupled plasma mass spectrometry. J. Anal. At. Spectrom. 10, 619–624. https://doi.org/10.1039/JA9951000619.

Hintelmann, H., Keppel-jones, K., Douglas Evans, R., 2000. Constants of mercury methylation and demethylation rates in sediments and comparison of tracer and ambient mercury availability. Environ. Toxicol. Chem. 19 (9), 2204–2211.

Hou, L., Xie, X., Wan, X., Kao, S.J., Jiao, N., Zhang, Y., 2018. Niche differentiation of ammonia and nitrite oxidizers along a salinity gradient from the Pearl River estuary to the South China Sea. Biogeosciences 15, 5169–5187. https://doi.org/10.5194/bg-15-5169-2018.

Jeffrey, S.W., Wright, S.W., Zapata, M., 2012. Microalgal classes and their signature pigments. In: Phytoplankton Pigments. Cambridge University Press, pp. 3–77. https://doi.org/10.1017/cbo9780511732263.004.

Lamborg, C.H., Hammerschmidt, C.R., Bowman, K.L., Swarr, G.J., Munson, K.M., Ohnemus, D.C., Lam, P.J., Heimbürger, L.E., Rijkenberg, M.J.A., Saito, M.A., 2014. A global ocean inventory of anthropogenic mercury based on water column measurements. Nature 512, 65–68. https://doi.org/10.1038/nature13563.

Lehnherr, I., St. Louis, V.L., Hintelmann, H., Kirk, J.L., 2011. Methylation of inorganic mercury in polar marine waters. Nat. Geosci. 4, 298–302. https://doi.org/10.1038/ngeo1134.

Lin, H., Ascher, D.B., Myung, Y., Lamborg, C.H., Hallam, S.J., Gionfriddo, C.M., Holt, K. E., Moreau, J.W., 2021. Mercury methylation by metabolically versatile and cosmopolitan marine bacteria. ISME J. 15, 1810–1825. https://doi.org/10.1038/s41396-020-00889-4.

Lomas, M.W., Lipschultz, F., 2006. Forming the primary nitrite maximum: nitrifiers or phytoplankton? Limnol. Oceanogr. 51 (5), 2453–2467.

Mason, R.P., Sullivan, K.A., 1999. The distribution and speciation of mercury in the South and equatorial Atlanic. Deep-Sea Res. II 46, 937–956.

Mason, R.P., Choi, A.L., Fitzgerald, W.F., Hammerschmidt, C.R., Lamborg, C.H., Soerensen, A.L., Sunderland, E.M., 2012. Mercury biogeochemical cycling in the ocean and policy implications. Environ. Res. 119, 101–117. https://doi.org/10.1016/j.envres.2012.03.013.

McIlvin, M.R., Altabet, M.A., 2005. Chemical conversion of nitrate and nitrite to nitrous oxide for nitrogen and oxygen isotopic analysis in freshwater and seawater. Anal. Chem. 77, 5589–5595. https://doi.org/10.1021/AC050528S.

Medeiros, P.M., Seidel, M., Ward, N.D., Carpenter, E.J., Gomes, H.R., Niggemann, J., Krusche, A.v., Richey, J.E., Yager, P.L., Dittmar, T., 2015. Fate of the Amazon River dissolved organic matter in the tropical Atlantic Ocean. Glob. Biogeochem. Cycles 29, 677–690. https://doi.org/10.1002/2015GB005115.

Mincer, T.J., Church, M.J., Taylor, L.T., Preston, C., Karl, D.M., DeLong, E.F., 2007. Quantitative distribution of presumptive archaeal and bacterial nitrifiers in Monterey Bay and the North Pacific Subtropical Gyre. Environ. Microbiol. 9, 1162–1175. https://doi.org/10.1111/j.1462-2920.2007.01239.x.

Monperrus, M., Tessier, E., Amouroux, D., Leynaert, A., Huonnic, P., Donard, O.F.X., 2007. Mercury methylation, demethylation and reduction rates in coastal and marine surface waters of the Mediterranean Sea. Mar. Chem. 107, 49–63. https://doi.org/10.1016/j.marchem.2007.01.018.

Montoya, J.P., Landrum, J.P., Weber, S.C., 2019. Amazon River influence on nitrogen fixation in the western tropical North Atlantic. The sea: the current and future ocean. J. Mar. Res. 77, 191–213.

Munson, K.M., Babi, D., Lamborg, C.H., 2014. Determination of monomethylmercury from seawater with ascorbic acid-assisted direct ethylation. Limnol. Oceanogr. Methods 12, 1–9. https://doi.org/10.4319/lom.2014.12.1.

Munson, K.M., Lamborg, C.H., Boiteau, R.M., Saito, M.A., 2018. Dynamic mercury methylation and demethylation in oligotrophic marine water. Biogeosciences 15, 6451–6460. https://doi.org/10.5194/bg-15-6451-2018.

Newell, S.E., Babbin, A.R., Jayakumar, A., Ward, B.B., 2011. Ammonia oxidation rates and nitrification in the Arabian Sea. Glob. Biogeochem. Cycles 25. https://doi.org/10.1029/2010GB003940.

Newell, S.E., Fawcett, S.E., Ward, B.B., 2013. Depth distribution of ammonia oxidation rates and ammonia-oxidizer community composition in the Sargasso Sea. Limnol. Oceanogr. 58, 1491–1500. https://doi.org/10.4319/lo.2013.58.4.1491.

Newell, S.E., McCarthy, M.J., Gardner, W.S., Fulweiler, R.W., 2016. Sediment nitrogen fixation: a call for re-evaluating coastal N budgets. Estuar. Coasts 39, 1626–1638. https://doi.org/10.1007/s12237-016-0116-y.

Ngugi, D., Blom, J., Stepanauskas, R., Stingl, U., 2016. Diversification and niche adaptations of *Nitrospina*-like bacteria in the polyextreme interfaces of Red Sea brines. ISME J. 10, 1383–1399.

Ortiz, V.L., Mason, R.P., Evan Ward, J., 2015. An examination of the factors influencing mercury and methylmercury particulate distributions, methylation and demethylation rates in laboratory-generated marine snow. Mar. Chem. 177, 753–762. https://doi.org/10.1016/j.marchem.2015.07.006.

Parks, J.M., Johs, A., Podar, M., Bridou, R., Hurt, R.A., Smith, S.D., Tomanicek, S.J., Qian, Y., Brown, S.D., Brandt, C.C., Palumbo, A.v, Smith, J.C., Wall, J.D., Elias, D.A., Liang, L., 2013. The genetic basis for bacterial mercury methylation. Science 1979 (339), 1332–1335.

Peña, M.A., Katsev, S., Oguz, T., Gilbert, D., 2010. Modeling dissolved oxygen dynamics and hypoxia. Biogeosciences 7, 933–957.

Podar, M., Gilmour, C.C., Brandt, C.C., Soren, Al, Brown, S.D., Crable, B.R., Palumbo, A. V., Somenahally, A.C., Elias, D.A., 2015. Global prevalence and distribution of genes and micoorganisms involved in mercury methylation. Sci. Adv. 1.

Santoro, A.E., Casciotti, K.L., Francis, C.A., 2010. Activity, abundance and diversity of nitrifying archaea and bacteria in the Central California Current. Environ. Microbiol. 12, 1989–2006. https://doi.org/10.1111/j.1462-2920.2010.02205.x.

Subramaniam, A., Yager, P.L., Carpenter, E.J., Mahaffey, C., Björkman, K., Cooley, S., Kustka, A.B., Montoya, J.P., Sañudo-Wilhelmy, S.A., Shipe, R., Capone, D.G., 2008. Amazon River enhances diazotrophy and carbon sequestration in the tropical North Atlanic Ocean. PNAS 105, 10460–10465, 10.1073pnas.0710279105.

Sunderland M., Elsie, Mason P., Robert, 2007. Human impacts on open ocean mercury concentrations. Glob. Biogeochem. Cycles 21, 1–15. https://doi.org/10.1029/2006gb002876.

Tada, Y., Marumoto, K., Takeuchi, A., 2020. Nitrospina-like Bacteria are potential mercury Methylators in the mesopelagic zone in the East China Sea. Front. Microbiol. 11 https://doi.org/10.3389/fmicb.2020.01369.

Tada, Y., Marumoto, K., Takeuchi, A., 2021. *Nitrospina* - like bacteria are dominant potential mercury methylators in both the Oyashio and Kuroshio regions of the Western North Pacific. Microbiol. Spectr. 9 (2).

Tolar, B.B., Wallsgrove, N.J., Popp, B.N., Hollibaugh, J.T., 2017. Oxidation of urea-derived nitrogen by thaumarchaeota-dominated marine nitrifying communities. Environ. Microbiol. 19, 4838–4850. https://doi.org/10.1111/1462-2920.13457.

Van Heukelem, L., Thomas, C., 2001. Computer-assisted high-performance liquid chromatography method development with applications to the isolation and analysis of phytoplankton pigments. J. Chromatogr. A 910.

Villar, E., Cabrol, L., Heimbürger-Boavida, L.E., 2020. Widespread microbial mercury methylation genes in the global ocean. Environ. Microbiol. Rep. 12, 277–287. https://doi.org/10.1111/1758-2229.12829.

Ward, B.B., Zafiriout, O.C., 1988. Nitrification and nitric oxide in the oxygen minimum of the eastern tropical North Pacific. Deep-Sea Res. 35, 1127–1142.

Whalin, L., Kim, E.H., Mason, R., 2007. Factors influencing the oxidation, reduction, methylation and demethylation of mercury species in coastal waters. Mar. Chem. 107, 278–294. https://doi.org/10.1016/j.marchem.2007.04.002.

Zhang, L., Wu, S., Zhao, L., Lu, X., Pierce, E.M., Gu, B., 2019. Mercury sorption and desorption on organo-mineral particulates as a source for microbial methylation. Environ. Sci. Technol. 53, 2426–2433. https://doi.org/10.1021/acs.est.8b06020.